European Journal of Chemistry

Design, synthesis, anticancer evaluation and molecular docking of new [V600E]BRAF inhibitors derived from pyridopyrazinone

Kamelia Mahmoud Amin [1], Ossama Metwally El-Badry [2], Doaa Ezzat Abdel Rahman [1], Usama Magdi Ammar [2,*] and Mohamed Mostafa Abdalla [3]

[1] *Pharmaceutical Chemistry Department, Faculty of Pharmacy, Cairo University, Cairo, 11562, Egypt*

[2] *Pharmaceutical Chemistry Department, Faculty of Pharmacy, Ahram Canadian University, Giza, 12566, Egypt*

[3] *Research Unit, Saco Pharma Company, 6th of October City, Egypt*

* Corresponding author at: Pharmaceutical Chemistry Department, Faculty of Pharmacy, Ahram Canadian University, Giza, 12566, Egypt.
Tel.: +20.02.38376751. Fax: +20.02.38334379. E-mail address: usama_acu@hotmail.com (U.M. Ammar).

ARTICLE INFORMATION

ABSTRACT

Design and synthesis of some new pyridopyrazinone derivatives as anti-proliferative agents is described. The cytotoxic activities of the synthesized compounds against melanoma cell line (LOXIMVI), ovarian cell line (OVCAR3), thyroid cell lines (CAL62, FTC133, BCPAP and ML1) and colon cell lines (HT29 and HCT116) were investigated. Results revealed that most compounds were active and compound 3d was the most active one. It exhibited promising activity against all tested cell lines. In addition, *in vitro* kinase assay against both [WT]BRAF and [V600E]BRAF was performed for all synthesized compounds. Furthermore, molecular docking of tested compounds was established with active site of [V600E]BRAF kinase domain. Results of kinase inhibition assay and molecular docking revealed that, compounds 1, 3d, e, h, i, 5d, e and 6b were potent inhibitors for [V600E]BRAF kinase enzyme involved in number of cancer types as melanoma, ovarian and thyroid cancer. The newly synthesized pyridopyrazinones substituted with different substituents at C-3 or fused with triazine heterocycle at C-3 and C-4 afforded potent [V600E]BRAF inhibitors and exhibited promising cytotoxic activities against different cancer types such as melanoma, ovarian, thyroid and colon cancer.

1. Introduction

Cancer is a group of diseases in which, three characteristic properties are involved related to the cancer cells: being aggressive, invasive, and possibility of metastasis [1]. It results from inter- and intra-cellular communication disorders, which can be originated from false messengers by hormones, cytokines, growth factors or false signal transduction generated by oncogenes [1].

G proteins, receptors tyrosine kinases (RTK) and non-receptor tyrosine kinases (NRTK) are considered important triggers of intracellular signal transduction of cell proliferation [2]. Rapidly growing fibrosarcoma (RAF) is considered a component of RTK that included the key mediators of carcinogenesis. Phosphorylation of RAF results in activation of extracellular signal-regulated kinase (ERK) that was translocated to nucleus to trigger cell proliferation and other biological process [3]. Three isoforms of RAF kinases; ARAF, BRAF, and CRAF were known [4]. BRAF mutation is highly involved in many cancer cells as melanoma (66%), thyroid cancer (35-70%), colorectal cancer (5-20%), liver cancer (14%), and ovarian cancer (30%) [5-11].

The most common mutation in BRAF among 95 BRAF mutations is [V600E]BRAF. [V600E]BRAF is a single base missense substitution (val 600 is replaced with glu in the activation loop) which is adjacent to phosphorylation target ser 599 during BRAF activation. The polarity of glutamic acid is similar to the phosphorylated serine in activation loop that led to rendering [V600E]BRAF active and resulted in uncontrolled cell growth [5,6,12,13]. Therefore, BRAF kinase is considered a critical therapeutic target in different types of cancer [14].

BRAF kinase enzyme inhibitors are classified into two categories; type I inhibitors, such as SB590885 (Figure 1), which bind to the BRAF kinase enzyme in its active conformation. Type II inhibitors, such as sorafenib (Figure 1), target that enzyme in its inactive conformation.

Biarylurea derivative, sorafenib was the first drug that target [V600E]BRAF in melanoma and exhibited *in vitro* inhibition only. It has no significant response in neither phase I nor phase II clinical trials [15-19]. Triarylimidazole derivative, SB590885, is considered a potent type I inhibitor of [V600E]BRAF *in vitro*, but had poor pharmacokinetic and pharmcodynamic profiles *in vivo* [20].
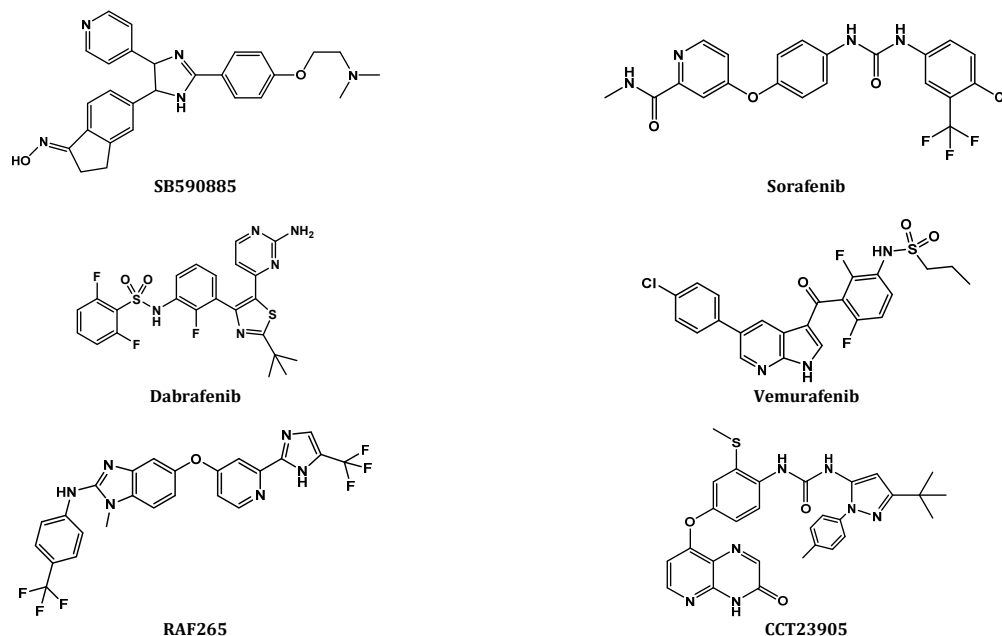
Figure 1. BRAF kinase inhibitors.

However, derivatives of pyrimidine, azaindole and benzimidazole such as darafenib, vemurafenib and RAF265, respectively, were involved in clinical trials as [V600E]BRAF kinase inhibitors [21] (Figure 1).

Pyridopyrazinone derivatives had considerable thera-peutic activities in the treatment of different cancer types as melanoma, thyroid, colon, and ovarian cancer through their selective inhibition of [V600E]BRAF [21]. Pyridopyrazinone derivatives were considered type II inhibitors of [V600E]BRAF, both *in vitro* and *in vivo*. Pyridopyrazinone activity was exhibited through selective binding with Cys 532 backbone of hinge region of [V600E]BRAF by hydrogen bonding [14,22]. CCT23905 was the first derivative of pyridopyrazinones described for inhibiting activity towards oncogenic BRAF [14].

Accordingly, new pyridopyrazinones were designed to be substituted with different substituents at C-3 or fused with another heterocycle at C-3 and C-4 to afford an additional binding sites that affect mode of interaction. These compounds were evaluated for their cytotoxic activity against different cancer cell lines. In addition, *in vitro* kinase assay was performed to evaluate their BRAF inhibition activities. Moreover, a molecular docking study was performed to assign the binding mode with active site of BRAF enzyme model.

2. Experimental

2.1. Chemistry

Melting points were determined by open capillary tube method using Gallen Kamp melting point apparatus MFB-595-010M (Gallen Kamp, London, England) and were uncorrected. Microanalysis was carried out at The Regional Center for Mycology and Biotechnology, Al-Azhar University. IR Spectra were recorded as potassium bromide discs on Schimadzu FT-IR 8400S spectrophotometer (Shimadzu, Kyoto, Japan) and expressed in wavenumber (ν) cm^{-1}. The ^{1}H NMR spectra were recorded on a Bruker NMR spectrometer at 400 MHz and Varian Mercury VX-300 NMR spectrometer at 300 MHz. Chemical Shifts are quoted in δ as parts per million (ppm) downfield from tetramethylsilane (TMS) as internal standard. Mass spectra were recorded using Shimadzu Gas Chroma-

tograph Mass spectrometer QP 1000 Ex (Shimadzu). TLC was carried out using Art. DC-Plastikfolien, Kieselgel 60F^{254} sheets (Merck, Darmstadt, Germany), the developing solvent was chloroform/methanol (9:1, *v:v*) and the spots were visualized at 366 and 254 nm by UV Vilber Lourmat 77202 (Vilber, Marne La Vallee, France).

2.1.1. Synthesis of 3-methylpyrido[2,3-b]pyrazin-2(1H)one (1)

Ethyl pyruvate (2.90 g, 2.77 mL, 0.025 mol) was added to a solution of 2,3-diaminopyridine (2.75 g, 0.025 mol) in ethanol (30 mL) and refluxed for 10 h. Reaction mixture was cooled, filtered, washed with ethanol (5 mL) and dried. The crude product was crystalized from ethanol (Scheme 1). Yield: 59%. M.p.: 278-280 °C. FT-IR (KBr, ν, cm^{-1}): 3186 (NH), 3018 (CH Ar), 2943, 2839 (CH Aliph), 1685 (C=O), 1641, 1631, 1597, 1559, 1546, 1527 (C=N, NH, C=C). ^{1}H NMR (300 MHz, DMSO-d_6, δ, ppm): 2.41 (s, 3H, CH$_3$), 7.48 (d, *J*= 8.4 Hz, 1H, H-8Ar), 7.67 (t, 1H, H-7Ar), 8.11 (d, *J*= 7.6 Hz, 1H, H-6Ar), 12.44 (s, 1H, NH, exchanged with D$_2$O). Anal. calcd. for C$_8$H$_7$N$_3$O: C, 59.62; H, 4.38; N, 26.07. Found: C, 59.90; H, 4.14; N, 26.73%.

2.1.2. Synthesis of 3-bromomethylpyrido[2,3-b]pyrazin-2 (1H)one (2)

Compound **1** (3.22 g, 0.02 mol) was dissolved in glacial acetic acid (10 mL) and anhydrous sodium acetate (1.64 g, 0.02 mol) was added. Bromine (3.04 g, 0.99 mL, 0.019 mol) was added dropwise and the mixture was heated on steam bath for 30 min. then cooled. The formed precipitate was filtered, washed with glacial acetic acid (5 mL) and dried. The crude product was crystalized from ethanol (Scheme 1). Yield: 43%. M.p.: 237-239 °C. FT-IR (KBr, ν, cm^{-1}): 3414 (NH), 3055 (CH Ar), 2980, 2883 (CH Aliph), 1670 (C=O), 1647, 1616, 1558, 1544, 1508 (C=N, NH, C=C). ^{1}H NMR (300 MHz, DMSO-d_6, δ, ppm): 3.10 (s, 2H, CH$_2$), 7.40 (d, *J* = 7.4 Hz, 1H, H-8Ar), 7.61 (t, 1H, H-7Ar), 8.35 (d, *J* = 6.1 Hz, 1H, H-6Ar), 11.50 (s, 1H, NH, exchanged with D$_2$O). MS (EI, *m/z* (%)): 240 (M$^+$, 0.53), 242 (M$^+$+2, 0.67). Anal. calcd. for C$_8$H$_6$BrN$_3$O: C, 40.03; H, 2.52; N, 17.50. Found: C, 40.13; H, 2.47; N, 17.68%.
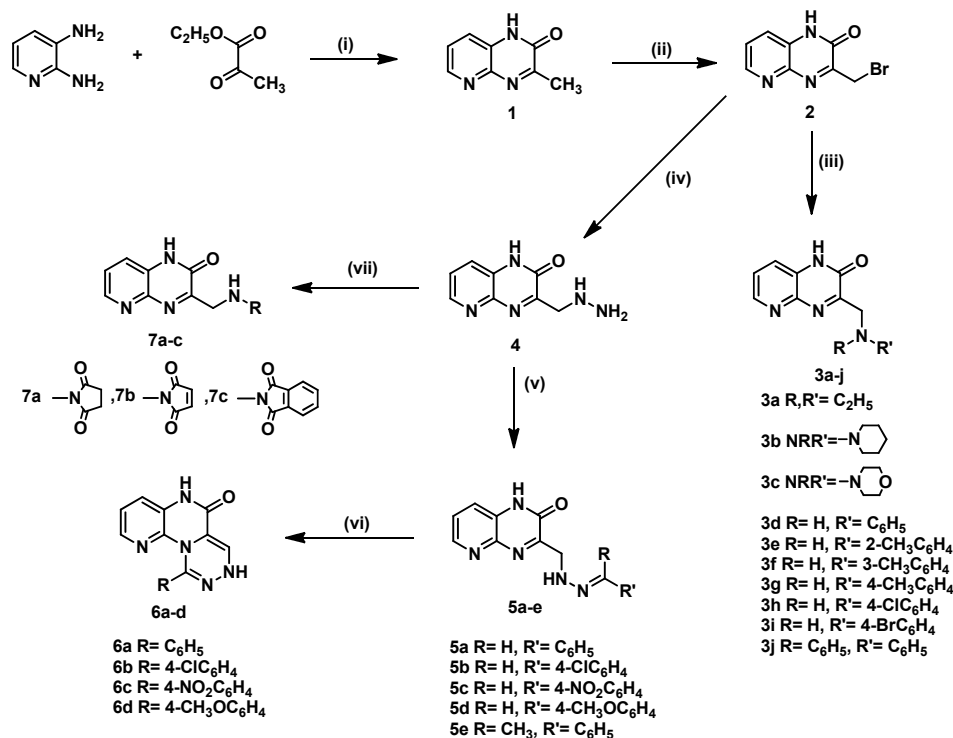
Reagents and conditions: (i) Ethanol, reflux, 10 h. (ii) Bromine, glacial acetic acid, anhydrous sodium acetate, reflux, 30 min. (iii) Appropriate amine, ethanol, sodium iodide, reflux, 10 h. (iv) Hydrazine hydrate, ethanol, reflux, 9 h. (v) Appropriate aldehyde or ketone, glacial acetic acid, reflux, 8 h. (vi) Bromine, glacial acetic acid, sodium acetate, room temp., 3 h. (vii) Appropriate cyclic acid anhydride, glacial acetic acid, reflux, 6 h.

Scheme 1

2.1.3. General procedure for synthesis of 3-substituted methylpyrido[2,3-b]pyrazin-2(1H)ones (3a-j)

Appropriate amine (0.02 mol) was added to a solution of compound **2** (2.4 g, 0.01 mol) in ethanol (30 mL) containing sodium iodide (0.15 g, 0.001 mol) and refluxed for 10 h. The reaction mixture was cooled, formed precipitate filtered, washed with ethanol (5 mL) and dried. The crude product was crystalized from ethanol (Scheme 1).

3-(N,N-Diethylamino)methylpyrido[2,3-b]pyrazin-2(1H)one (**3a**): Yield: 81%. M.p.: 262-263 °C. FT-IR (KBr, ν, cm⁻¹): 3238 (NH), 3051 (CH Ar), 2924, 2852 (CH Aliph), 1672 (C=O), 1637, 1624, 1612, 1593, 1508 (C=N, NH, C=C). ¹H NMR (300 MHz, DMSO-d_6, δ, ppm): 1.41 (t, 6H, 2xCH₂C*H₃*), 2.29 (q, 4H, 2x C*H₂*CH₃), 2.43 (s, 2H, CH₂), 7.11 (d, J = 7.4 Hz, 1H, H-8Ar), 7.30 (t, 1H, H-7Ar), 8.21 (d, J = 6.4 Hz, 1H, H-6Ar), 10.80 (s, 1H, NH, exchanged with D₂O). Anal. calcd. for C₁₂H₁₆N₄O: C, 62.05; H, 6.94; N, 24.12. Found: C, 62.18; H, 6.97; N, 24.13%.

3-(Piperidin-1-yl)methylpyrido[2,3-b]pyrazin-2(1H)one (**3b**): Yield: 80%. M.p.: 277-279 °C. FT-IR (KBr, ν, cm⁻¹): 3387 (NH), 3066 (CH Ar), 2964, 2866 (CH Aliph), 1700 (C=O), 1649, 1612, 1591, 1508, 1500 (C=N, NH, C=C). ¹H NMR (300 MHz, DMSO-d_6, δ, ppm): 2.06-2.32 (m, 10H, piperidine H), 2.51 (s, 2H, CH₂), 7.31 (d, J = 8.0 Hz, 1H, H-8Ar), 7.53 (t, 1H, H-7Ar), 8.22 (d, J = 6.6 Hz, 1H, H-6Ar), 11.13 (s, 1H, NH, exchanged with D₂O). Anal. calcd. for C₁₃H₁₆N₄O: C, 63.91; H, 6.60; N, 22.93. Found: C, 63.98; H, 6.64; N, 23.10%.

3-(Morpholin-4-yl)methylpyrido[2,3-b]pyrazin-2(1H)one (**3c**): Yield: 74%. M.p.: 234-235 °C. FT-IR (KBr, ν, cm⁻¹): 3394 (NH), 3059 (CH Ar), 2920, 2840 (CH Aliph), 1674 (C=O), 1640, 1618, 1593, 1580, 1540 (C=N, NH, C=C). ¹H NMR (300 MHz, DMSO-d_6, δ, ppm): 2.04 (t, 4H, morpholine H), 2.41 (s, 2H, CH₂), 3.30 (t, 4H, morpholine H), 7.33 (d, J = 8.0 Hz, 1H, H-8Ar), 7.75 (t, 1H, H-7Ar), 8.12 (d, J = 7.4 Hz, 1H, H-6Ar), 10.89 (s, 1H, NH, exchanged with D₂O). Anal. calcd. for C₁₂H₁₄N₄O₂: C, 58.53; H, 5.73; N, 22.75. Found: C, 58.61; H, 5.71; N, 22.92%.

3-Phenylaminomethylpyrido[2,3-b]pyrazin-2(1H)one (**3d**): Yield: 60%. M.p.: 248-250 °C. FT-IR (KBr, ν, cm⁻¹): 3404, 3385 (2NH), 3049 (CH Ar), 2926, 2852 (CH Aliph), 1672 (C=O), 1593, 1560, 1521, 1508 (C=N, NH, C=C). ¹H NMR (400 MHz, DMSO-d_6, δ, ppm): 3.10 (s, 2H, CH₂), 6.52-7.10 (m, 5H, H-2', 3', 4', 5', 6' Ar), 7.21 (d, J = 9.6 Hz, 1H, H-8Ar), 7.50 (t, 1H, H-7Ar), 8.17 (d, J = 8.2 Hz, 1H, H-6Ar), 10.62 (s, 1H, NH, exchanged with D₂O), 11.51 (s, 1H, NH, exchanged with D₂O). Anal. calcd. for C₁₄H₁₂N₄O: C, 66.65; H, 4.79; N, 22.21. Found: C, 66.83; H, 4.74; N, 22.37%.

3-(2-Methylphenyl)aminomethylpyrido[2,3-b]pyrazin-2(1H) one (**3e**): Yield: 64%. M.p.: 296-298 °C. FT-IR (KBr, ν, cm⁻¹): 3414, 3385 (2NH), 3049 (CH Ar), 2924, 2854 (CH Aliph), 1672 (C=O), 1649, 1622, 1593, 1570, 1521 (C=N, NH, C=C). ¹H NMR (400 MHz, DMSO-d_6, δ, ppm): 2.13 (s, 3H, CH₃), 3.11 (s, 2H, CH₂), 6.30-7.00 (m, 4H, H-3', 4', 5', 6' Ar), 7.21 (d, J = 7.2 Hz, 1H, H-8Ar), 7.50 (t, 1H, H-7Ar), 8.16 (d, J = 8.4 Hz, 1H, H-6Ar), 10.80 (s, 1H, NH, exchanged with D₂O), 11.44 (s, 1H, NH, exchanged with D₂O). Anal. calcd. for C₁₅H₁₄N₄O: C, 67.65; H, 5.30; N, 21.04. Found: C, 67.82; H, 5.32; N, 21.08%.

3-(3-Methylphenyl)aminomethylpyrido[2,3-b]pyrazin-2(1H) one (**3f**): Yield: 57%. M.p.: 258-260 °C. FT-IR (KBr, ν, cm⁻¹): 3414, 3388 (2NH), 3057 (CH Ar), 2922, 2852 (CH Aliph), 1674 (C=O), 1622, 1593, 1558, 1518 (C=N, NH, C=C). ¹H NMR (400 MHz, DMSO-d_6, δ, ppm): 2.15 (s, 3H, CH₃), 3.32 (s, 2H, CH₂), 6.12-6.99 (m, 4H, H-2', 4', 5', 6' Ar), 7.20 (d, J = 6.3 Hz, 1H, H-8Ar), 7.50 (t, 1H, H-7Ar), 8.19 (d, J = 8.3 Hz, 1H, H-6Ar), 10.81 (s, 1H, NH, exchanged with D₂O), 11.50 (s, 1H, H NH, exchanged with D₂O). Anal. calcd. for C₁₅H₁₄N₄O: C, 67.65; H, 5.30; N, 21.04. Found: C, 67.84; H, 5.34; N, 21.06%.

3-(4-Methylphenyl)aminomethylpyrido[2,3-b]pyrazin-2(1H) one (**3g**): Yield: 73%. M.p.: 284-286 °C. FT-IR (KBr, ν, cm⁻¹): 3369, 3350 (2NH), 3051 (CH Ar), 2926, 2856 (CH Aliph), 1672 (C=O), 1612, 1591, 1544, 1514 (C=N, NH, C=C). ¹H NMR (300 MHz, DMSO-*d*₆, δ, ppm): 2.10 (s, 3H, CH₃), 2.41 (s, 2H, CH₂), 6.30-6.83 (m, 4H, H-2', 3', 5', 6' Ar), 7.22 (d, *J* = 6.7 Hz, 1H, H-8Ar), 7.54 (t, 1H, H-7Ar), 8.17 (d, *J* = 7.0 Hz, 1H, H-6Ar), 10.09 (s, 1H, NH, exchanged with D₂O), 11.51 (s, 1H, NH, exchanged with D₂O). Anal. calcd. for C₁₅H₁₄N₄O: C, 67.65; H, 5.30; N, 21.04. Found: C, 67.80; H, 5.30; N, 21.18%.

3-(4-Chlorophenyl)aminomethylpyrido[2, 3-b]pyrazin-2(1H) one (**3h**): Yield: 66%. M.p.: >300 °C. FT-IR (KBr, ν, cm⁻¹): 3421, 3385 (2NH), 3093 (CH Ar), 2924, 2852 (CH Aliph), 1674 (C=O), 1647, 1624, 1593, 1570 (C=N, NH, C=C). ¹H NMR (400 MHz, DMSO-*d*₆, δ, ppm): 3.31 (s, 2H, CH₂), 6.42-7.12 (m, 4H, H-2', 3', 5', 6' Ar), 7.21 (d, *J* = 6.3 Hz, 1H, H-8Ar), 7.59 (t, 1H, H-7Ar), 8.11 (d, *J* = 6.2 Hz, 1H, H-6Ar), 11.00 (s, 1H, NH, exchanged with D₂O), 11.59 (s, 1H, NH, exchanged with D₂O). Anal. calcd. for C₁₄H₁₁ClN₄O: C, 58.65; H, 3.87; N, 19.54. Found: C, 58.78; H, 3.92; N, 19.73%.

3-(4-Bromophenyl)aminomethylpyrido[2,3-b]pyrazin-2(1H) one (**3i**): Yield: 79%. M.p.: >300 °C. FT-IR (KBr, ν, cm⁻¹): 3400, 3388 (2NH), 3101 (CH Ar), 2924, 2897 (CH Aliph), 1664 (C=O), 1649, 1618, 1593 (C=N, NH, C=C). ¹H NMR (400 MHz, DMSO-*d*₆, δ, ppm): 3.11 (s, 2H, CH₂), 6.36-7.20 (m, 4H, H-2', 3', 5', 6' Ar), 7.41 (d, *J* = 8.1 Hz, 1H, H-8Ar), 7.69 (t, 1H, H-7Ar), 8.22 (d, *J* = 6.0 Hz, 1H, H-6Ar), 11.02 (s, 1H, NH, exchanged with D₂O), 11.61 (s, 1H, NH, exchanged with D₂O). Anal. calcd. for C₁₄H₁₁BrN₄O: C, 50.77; H, 3.35; N, 16.92. Found: C, 50.91; H, 3.37; N, 16.98%.

3-(N,N-Diphenylamino)methylpyrido[2, 3-b]pyrazin-2(1H) one (**3j**): Yield: 46%. M.p.: 292-293 °C. FT-IR (KBr, ν, cm⁻¹): 3410 (NH), 3057 (CH Ar), 2924, 2852 (CH Aliph), 1662 (C=O), 1649, 1610, 1591, 1570, 1508 (C=N, NH, C=C). ¹H NMR (400 MHz, DMSO-*d*₆, δ, ppm): 3.32 (s, 2H, CH₂), 6.50-7.11 (m, 10H, Ar H), 7.21 (d, *J* = 7.2 Hz, 1H, H-8Ar), 7.55 (t, 1H, H-7Ar), 8.15 (d, *J* = 7.0 Hz, 1H, H-6 Ar), 11.44 (s, 1H, NH, exchanged with D₂O). Anal. calcd. for C₂₀H₁₆N₄O: C, 73.15; H, 4.91; N, 17.06. Found: C, 73.28; H, 4.97; N, 17.22%.

2.1.4. Synthesis of 3-Hydrazinomethylpyrido[2,3-b]pyrazin-2(1H)one (4)

Hydrazine hydrate (7.00 g, 6.86 mL, 0.14 mol) was added to a solution of compound **2** (2.40 g, 0.01 mol) in ethanol (20 mL) and refluxed for 9 h. The mixture was cooled in ice bath for 10 min. and formed precipitate was filtered. The precipitate was washed with ethanol (5 mL) and dried. The crude product was crystallized from ethanol (Scheme 1). Yield: 73%. M.p.: 243-245 °C. FT-IR (KBr, ν, cm⁻¹): 3369, 3329 (NH₂, 2NH), 3066 (CH Ar), 2924, 2852 (CH Aliph), 1670 (C=O), 1612, 1591, 1570, 1508 (C=N, NH, C=C). ¹H NMR (400 MHz, DMSO-*d*₆, δ, ppm): 2.51 (s, 2H, CH₂), 7.21 (d, *J* = 6.2 Hz, 1H, H-8Ar), 7.50 (t, 1H, H-7Ar), 8.22 (d, *J* = 8.2 Hz, 1H, H-6Ar), 10.72 (s, 1H, NH, exchanged with D₂O), 11.22 (s, 2H, NH₂, exchanged with D₂O), 11.50 (s, 1H, NH, exchanged with D₂O). Anal. calcd. for C₈H₉N₅O: C, 50.26; H, 4.74; N, 36.63. Found: C, 50.41; H, 4.73; N, 37.01%.

2.1.5. General procedure for synthesis of 3-(2-(un)substituted benzylidene)hydrazinomethylpyrido[2,3-b]pyrazin-2(1H)-ones (5a-e)

Appropriate aromatic aldehyde or ketone (0.01 mol) was added to a solution of compound **4** (1.91 g, 0.01 mol) in glacial acetic acid (10 mL) and refluxed for 8 h. The mixture was allowed to cool then poured onto crushed ice (30 g). The precipitate was filtered, washed with water (5 mL) and dried. The crude product was crystallized from ethanol (Scheme 1).

3-(2-Benzylidene)hydrazinomethylpyrido[2, 3-b]pyrazin-2 (1H)-one (**5a**): Yield: 62%. M.p.: 234-236 °C. FT-IR (KBr, ν, cm⁻¹): 3398, 3364 (2NH), 3061 (CH Ar), 2901, 2829 (CH Aliph), 1676 (C=O), 1624, 1600, 1583, 1544, 1508 (C=N, NH, C=C). ¹H NMR (400 MHz, DMSO-*d*₆, δ, ppm): 2.32 (s, 2H, CH₂), 7.21 (d, *J* = 7.2 Hz, 1H, H-8 Ar), 7.31-7.42 (m, 3H, H-3',4',5' Ar), 7.45 (t, 1H, H-7 Ar), 7.62 (d, *J* = 6.7 Hz, 2H, H-2',6' Ar), 8.11 (s, 1H, N=CH), 8.22 (d, *J* = 6.2 Hz, 1H, H-6Ar), 11.32 (s, 1H, NH, exchanged with D₂O), 11.54 (s, 1H, NH, exchanged with D₂O). Anal. calcd. for C₁₅H₁₃N₅O: C, 64.51; H, 4.69; N, 25.07. Found: C, 64.67; H, 4.73; N, 25.19%.

3-[2-(4-Chlorobenzylidene)]hydrazinomethylpyrido[2, 3-b] pyrazin-2(1H)-one (**5b**): Yield: 69%. M.p.: 237-239 °C. FT-IR (KBr, ν, cm⁻¹): 3421, 3387 (2NH), 3012 (CH Ar), 2920, 2837 (CH Aliph), 1683 (C=O), 1616, 1593, 1558, 1541, 1521 (C=N, NH, C=C). ¹H NMR (400 MHz, DMSO-*d*₆, δ, ppm): 2.42 (s, 2H, CH₂), 7.22 (d, *J* = 7.3 Hz, 1H, H-8 Ar), 7.34 (d, *J* = 6.1 Hz, 2H, H-3',5' Ar), 7.46 (t, 1H, H-7Ar), 7.59 (d, *J* = 7.0 Hz, 2H, H-2',6' Ar), 8.11 (s, 1H, N=CH), 8.22 (d, *J* = 6.3 Hz, 1H, H-6 Ar), 11.30 (s, 1H, NH, exchanged with D₂O), 11.51 (s, 1H, NH, exchanged with D₂O). MS (EI, *m/z* (%)): 313 (M⁺, 2.63), 315 (M⁺+2, 2.77). Anal. calcd. for C₁₅H₁₂ClN₅O: C, 57.42; H, 3.86; N, 22.32. Found: C, 57.52; H, 3.91; N, 22.48%.

3-[2-(4-Nitrobenzylidene)]hydrazinomethylpyrido[2, 3-b] pyrazin-2(1H)-one (**5c**): Yield: 70%. M.p.: 238-240 °C. FT-IR (KBr, ν, cm⁻¹): 3444, 3365 (2NH), 3021 (CH Ar), 2926, 2850 (CH Aliph), 1677 (C=O), 1653, 1614, 1597, 1558 (C=N, NH, C=C), 1519, 1344 (NO₂). ¹H NMR (400 MHz, DMSO-*d*₆, δ, ppm): 2.33 (s, 2H, CH₂), 7.21 (d, *J* = 6.4 Hz, 1H, H-8Ar), 7.66 (t, 1H, H-7Ar), 7.91-8.10 (m, 4H, H-2', 3', 5', 6' Ar), 8.19 (s, 1H, N=CH), 8.23 (d, *J* = 7.2 Hz, 1H, H-6Ar), 11.32 (s, 1H, NH, exchanged with D₂O), 11.50 (s, 1H, NH, exchanged with D₂O). Anal. calcd. for C₁₅H₁₂N₆O₃: C, 55.55; H, 3.73; N, 25.91. Found: C, 55.74; H, 3.74; N, 26.07%.

3-[2-(4-Methoxybenzylidene)]hydrazinomethylpyrido[2, 3-b]pyrazin-2(1H)-one (**5d**): Yield: 63%. M.p.: 256-258 °C. FT-IR (KBr, ν, cm⁻¹): 3417, 3392 (2NH), 3039 (CH Ar), 2933, 2837 (CH Aliph), 1670 (C=O), 1598, 1575, 1558, 1541, 1508 (C=N, NH, C=C). ¹H NMR (400 MHz, DMSO-*d*₆, δ, ppm): 2.12 (s, 2H, CH₂), 3.52 (s, 3H, OCH₃), 6.76 (d, *J* = 8.2 Hz, 2H, H-3',5' Ar), 7.21 (d, *J* = 7.1 Hz, 1H, H-8 Ar), 7.43 (t, 1H, H-7 Ar), 7.66 (d, *J* = 7.4 Hz, 2H, H-2',6' Ar), 8.10 (s, 1H, N=CH), 8.22 (d, *J* = 7.6 Hz, 1H, H-6Ar), 11.30 (s, 1H, NH, exchanged with D₂O), 11.45 (s, 1H, NH, exchanged with D₂O). Anal. calcd. for C₁₆H₁₅N₅O₂: C, 62.13; H, 4.89; N, 22.64. Found: C, 62.26; H, 4.87; N, 22.72%.

3-(2-Methyl-2-phenyl)hydrazinomethylpyrido[2, 3-b]pyrazin -2(1H)-one (**5e**): Yield: 69%. M.p.: 230-233 °C. FT-IR (KBr, ν, cm⁻¹): 3446, 3363 (2NH), 3032 (CH Ar), 2929, 2856 (CH Aliph), 1670 (C=O), 1645, 1616, 1570, 1558, 1521, (C=N, NH, C=C). ¹H NMR (400 MHz, DMSO-*d*₆, δ, ppm): 1.42 (s, 3H, CH₃), 2.50 (s, 2H, CH₂), 7.22 (d, *J* = 6.2 Hz, 1H, H-8Ar), 7.30-7.43 (m, 3H, H-3',4',5' Ar), 7.49 (t, 1H, H-7Ar), 7.63 (d, *J* = 8.1 Hz, 2H, H-2',6' Ar), 8.22 (d, *J* = 7.2 Hz, 1H, H-6Ar), 11.31 (s, 1H, NH, exchanged with D₂O), 11.53 (s, 1H, NH, exchanged with D₂O). Anal. calcd. for C₁₆H₁₅N₅O: C, 65.52; H, 5.15; N, 23.88. Found: C, 65.59; H, 5.12; N, 23.98%.

2.1.6. General procedure for synthesis of 4-(un)substituted phenyl-2,5,10,11-tetrahydropyrido[2,3-g]pyrazino[4,3-e] 1,2,4-triazin-11-ones (6a-d)

Bromine (1.60 g, 0.53 mL, 0.01 mol) in glacial acetic acid (0.6 mL) was added dropwise to solution of compound **5a-d** (0.01 mol) in glacial acetic acid (9 mL) containing sodium acetate (2.46 g, 0.03 mol) at room temperature. The mixture was stirred for 3 h at room temperature then poured onto cold water (50 mL). The formed precipitate was filtered, washed with water (10 mL) and dried. The crude product was crystallized from acetic acid (Scheme 1).

4-Phenyl-2,5,10,11-tetrahydropyrido[2, 3-g]pyrazino[4, 3-e] 1,2,4-triazin-11-one (**6a**): Yield: 80%. M.p.: 219-221 °C. FT-IR (KBr, ν, cm^{-1}): 3365, 3355 (2NH), 3035 (CH Ar), 1760 (C=O), 1608, 1558, 1541, 1521, 1508 (C=N, NH, C=C). ^{1}H NMR (400 MHz, DMSO-d_6, δ, ppm): 6.01 (s, 1H, H-1 Ar), 6.99 (t, 1H, H-8 Ar), 7.01 (d, J = 6.4 Hz, 1H, H-9 Ar), 7.29-7.41 (m, 3H, H-3',4',5' Ar), 7.63 (d, J = 7.2 Hz, 2H, H-2',6' Ar), 7.91 (d, J = 6.0 Hz, 1H, H-7 Ar),11.29 (s, 1H, NH, , exchanged with D$_2$O), 11.52 (s, 1H, exchanged with D$_2$O). Anal. calcd. for C$_{15}$H$_{11}$N$_5$O: C, 64.97; H, 4.00; N, 25.13. Found: C, 65.13; H, 4.06; N, 25.49%.

4-(4-Chlorophenyl)-2, 5, 10, 11-tetrahydropyrido[2, 3-g] pyrazino[4,3-e]1,2,4-triazin-11-one (**6b**): Yield: 75%. M.p.: 222-225 °C. FT-IR (KBr, ν, cm^{-1}): 3390, 3385 (2NH), 3032 (CH Ar), 1680 (C=O), 1635, 1608, 1593, 1570, 1558 (C=N, NH, C=C). ^{1}H NMR (400 MHz, DMSO-d_6, δ, ppm): 5.99 (s, 1H, H-1 Ar), 6.86 (t, 1H, H-8 Ar), 7.02 (d, J = 8.1 Hz, 1H, H-9 Ar), 7.33 (d, J = 7.0 Hz, 2H, H-3',5' Ar), 7.62 (d, J = 6.5 Hz, 2H, H-2',6' Ar), 8.22 (d, J = 6.3 Hz, 1H, H-7 Ar), 11.31 (s, 1H, NH, exchanged with D$_2$O), 11.53 (s, 1H, NH, exchanged with D$_2$O). Anal. calcd. for C$_{15}$H$_{10}$ClN$_5$O: C, 57.79; H, 3.23; N, 22.47. Found: C, 57.96; H, 3.19; N, 22.63%.

4-(4-Nitrophenyl)-2, 5, 10, 11-tetrahydropyrido[2, 3-g] pyrazino[4,3-e]1,2,4-triazin-11-one (**6c**): Yield: 86%. M.p.: 222-224 °C. FT-IR (KBr, ν, cm^{-1}): 3410, 3393 (2NH), 3041 (CH Ar), 1674 (C=O), 1654, 1635, 1600, 1568, 1558 (C=N, NH, C=C), 1521, 1346 (NO$_2$). ^{1}H NMR (400 MHz, DMSO-d_6, δ, ppm): 6.21 (s, 1H, H-1 Ar), 6.62 (t, 1H, H-8 Ar), 6.84 (d, J = 7.2 Hz, 1H, H-9 Ar), 7.56 (d, J = 8.1 Hz, 1H, H-7Ar), 7.91-8.10 (m, 4H, H-2', 3', 5', 6' Ar), 11.33 (s, 1H, NH, exchanged with D$_2$O), 11.50 (s, 1H, NH, exchanged with D$_2$O). Anal. calcd. for C$_{15}$H$_{10}$N$_6$O$_3$: C, 55.90; H, 3.13; N, 26.08. Found: C, 56.03; H, 3.17; N, 26.32%.

4-(4-Methoxyphenyl)-2, 5, 10, 11-tetrahydropyrido[2,3-g] pyrazino[4,3-e]1,2,4-triazin-11-one (**6d**): Yield: 66%. M.p.: 229-231 °C. FT-IR (KBr, ν, cm^{-1}): 3415, 3388 (2NH), 3020 (CH Ar), 2933, 2841 (CH Aliph), 1674 (C=O), 1633, 1597, 1575, 1558, 1508 (C=N, NH, C=C). ^{1}H NMR (300 MHz, DMSO-d_6, δ, ppm): 3.72 (s, 3H, OCH$_3$), 5.82 (s, 1H, H-1 Ar), 6.54 (t, 1H, H-8 Ar), 6.96 (d, J = 6.0 Hz, 1H, H-9 Ar), 7.03-7.40 (m, 4H, H-2', 3', 5', 6' Ar), 7.67 (d, J = 7.3 Hz, 1H, H-7 Ar), 11.33 (s, 1H, NH, exchanged with D$_2$O), 11.51 (s, 1H, NH, exchanged with D$_2$O).

2.1.7. General procedure for synthesis of 3-(2,5-dioxopyrrol (or pyroliden)-1-yl)aminomethylpyrido[2,3-b]pyrazin-2 (1H)ones (7a-c)

Appropriate cyclic acid anhydride (0.005 mol) was added to solution of hydrazine compound **4** (0.96 g, 0.005 mol) in glacial acetic acid (10 mL) and refluxed for 6 h. After cooling, the mixture was poured onto crushed ice (30 g). The formed precipitate was filtered, washed with water (5 mL) and dried. The crude product was crystalized from ethanol (Scheme 1).

3-(2, 5-Dioxopyrroliden-1-yl)aminomethylpyrido[2, 3-b] pyrazin-2(1H)one (**7a**): Yield: 86%. M.p.: 215-217 °C. FT-IR (KBr, ν, cm^{-1}): 3410, 3396 (2NH), 3026 (CH Ar), 2962, 2848 (CH Aliph), 1668 (3C=O), 1635, 1602, 1589, 1558, 1521 (C=N, NH, C=C). ^{1}H NMR (300 MHz, DMSO-d_6, δ, ppm): 2.56 (s, 2H, CH$_2$), 3.11 (t, 4H, CH$_2$-CH$_2$), 7.22 (d, J = 6.1 Hz, 1H, H-8Ar), 7.58 (t, 1H, H-7Ar), 8.18 (d, J = 6.4 Hz, 1H, H-6Ar), 11.23 (s, 1H, NH, exchanged with D$_2$O), 11.44 (s, 1H, NH, exchanged with D$_2$O). Anal. calcd. for C$_{12}$H$_{11}$N$_5$O$_3$: C, 52.75; H, 4.06; N, 25.63. Found: C, 52.84; H, 4.11; N, 25.89%.

3-(2,5-Dioxo-2,5-dihydro-1H-pyrrol-1-yl)aminomethylpyrido [2,3-b]pyrazin-2(1H)one (**7b**): Yield: 85%. M.p.: 212-215 °C. FT-IR (KBr, ν, cm^{-1}): 3421, 3398 (2NH), 3030 (CH Ar), 2964, 2848 (CH Aliph). ^{1}H NMR (400 MHz, DMSO-d_6, δ, ppm): 2.55 (s, 2H, CH$_2$), 5.11 (d, J = 8.7 Hz, 2H, CH=CH), 7.21 (d, J = 6.3 Hz, 1H, H-8Ar), 7.50 (t, 1H, H-7Ar), 8.01 (d, J = 7.7 Hz, 1H, H-6Ar), 11.33 (s, 1H, NH, exchanged with D$_2$O), 11.49 (s, 1H, NH,

exchanged with D$_2$O). Anal. calcd. for C$_{12}$H$_9$N$_5$O$_3$: C, 53.14; H, 3.34; N, 25.82. Found: C, 53.22; H, 3.31; N, 26.04%.

3-(2, 5-Dioxo-2, 5-dihydro-1H-benzo[c]pyrrol-1-yl)amino methylpyrido[2,3-b]pyrazin-2(1H)one (**7c**): Yield: 86%. M.p.: 218-221 °C. FT-IR (KBr, ν, cm^{-1}): 3446, 3395 (2NH), 3010 (CH Ar), 2966, 2854 (CH Aliph), 1683 (3C=O), 1637, 1602, 1587, 1568, 1541, 1521 (C=N, NH, C=C). ^{1}H NMR (400 MHz, DMSO-d_6, δ, ppm): 2.70 (s, 2H, CH$_2$), 7.22 (d, J = 6.2 Hz, 1H, H-8Ar), 7.46 (t, 1H, H-7Ar), 7.66-8.01 (m, 4H, H-3', 4', 5', 6' Ar), 8.26 (d, J = 8.0 Hz, 1H, H-6 Ar), 11.33 (s, 1H, NH, exchanged with D$_2$O), 11.55 (s, 1H, NH, exchanged with D$_2$O). Anal. calcd. for C$_{16}$H$_{11}$N$_5$O$_3$: C, 59.81; H, 3.45; N, 21.80. Found: C, 59.97; H, 3.52; N, 22.04%.

2.2. Biological activity

2.2.1. Antitumor screening

The cytotoxicity of the newly synthesized compounds was performed against different cancer cell lines, melanoma cell line (LOXIMVI), ovarian cell line (OVCAR3), thyroid cell lines (CAL62, FTC133, BCPAP and ML1) and colon cell lines (HT29 and HCT116), with the MTT assay according to the Mosmann's method [23]. The cells used in cytotoxicity assay were cultured in RPMI 1640 medium supplemented with 10% fetal calf serum. Cells suspended in the medium (2×10^4/mL) were plated in 96-well culture plates and incubated at 37°C in a 5% CO$_2$ incubator. After 12 h, the test sample (2 μL) was added to the cells (2×10^4) in 96-well plates and cultured at 37°C for 3 days. The cultured cells were mixed with 20 μL of MTT solution and incubated for 4 h at 37°C. The supernatant was carefully removed from each well and 100 μL of DMSO were added to each well to dissolve the formazan crystals which were formed by the cellular reduction of MTT. After mixing with a mechanical plate mixer, the absorbance of each well was measured by a microplate reader using a test wavelength of 570 nm [24]. The results were expressed as the IC$_{50}$ [23], which inducing a 50% inhibition of cell growth of treated cells when compared to the growth of control cells. Each experiment was performed at least 3 times. The concentration ranges used were 0.00001, 0.00005, 0.0001, 0.0005, 0.001, 0.005, 0.01, 0.05, 0.1, 0.5, 1, 5 and 10 μM. There was a good reproducibility between replicate wells with standard errors below 10%.

2.2.2. In vitro kinase assay

2.2.2.1. Protein expression and purification

Human BRAF kinase domain, BRAF-KD (residues 433-726) with an N-terminal purification tag (MDRGSH$_6$GS), and full-length mouse p50^{cdc37} were cloned into a pFastBac Dual vector. BRAF wild-type and V600E mutant kinase domains were expressed and purified. Briefly, Sf9 cells infected with the BRAF kinase domain harboring baculo virus were re-suspended in sonication buffer for sonication, and the lysate was cleared by high-speed centrifugation. Equilibrated Talon resin was added into the cleared lysate; the resin was washed with 10 column volumes of wash buffer (25 mM Tris (pH = 8.0), 250 mM NaCl, 5 mM imidazole, and 10% glycerol) and then eluted with addition of buffer (25 mM Tris (pH = 7.0), 250 mM NaCl, 160 mM imidazole, and 10% glycerol). The eluant from the Talon resin was diluted 3-fold and loaded on a SP resin column. SP resin was extensively washed (25 mM Tris (pH = 8.0), 50 mM NaCl, 1 mM dithiothreitol, and 10% glycerol) and eluted with high-salt buffer (25 mM Tris (pH = 8.0), 500 mM NaCl, 1 mM dithiothreitol, 1 mM EDTA, and 10% glycerol). Recombinantly expressed λ phosphatase was then added to the SP eluant and incubated for 2 h at room temperature followed by 7-fold dilution in buffer (25 mM Tris (pH = 8.0), 1 mM dithiothreitol, 1 mM EDTA, and 10%

glycerol). This dilution was reloaded on an SP resin column to remove the λ phosphatase. The final SP eluant was concentrated and loaded onto a Superdex 200 gel filtration column equilibrated in buffer (25 mM Tris (pH = 8.0), 300 mM NaCl, 1 mM dithiothreitol, 1 mM EDTA, and 5% glycerol). Gel filtration fractions were concentrated with a final glycerol concentration of 15% to a protein concentration of 1.5 mg/mL. BRAF-KD protein was immediately used for crystallization.

GST-MEK-His protein was overexpressed at 37 °C in *Escherichia coli* BL21 (Gold) cells (Invitrogen) in LB medium until the OD value reached 0.4-0.6. Isopropyl 1-thio-β-D-galactopyrano-side (IPTG, 0.5 mM) was then added to the culture, which was grown at 15 °C for an additional 16 h. The cell pellet was re-suspended and sonicated in sonication buffer (20 mM HEPES (4-(2-hydroxyethyl)-1-piperazineethane sulfonic acid)) (pH = 7.5), 500 mM NaCl, 10 mM 2-mercapto ethanol (BME), 10 mM imidazole, 0.1 mg/mL phenylmethane sulfonyl fluoride (PMSF), and 5% glycerol). The lysate was cleared by high speed centrifugation before it was loaded onto a Ni-NTA resin column pre-equilibrated in sonication buffer. The protein-bound Ni-NTA resin was then extensively washed with 20 column volumes of wash buffer, and the GST-MEK-His protein was eluted with an imidazole gradient from 10 to 150 mM in wash buffer. Fractions corresponding to GST-MEK-His were pooled and applied to a Superdex 200 column equilibrated in buffer (20 mM HEPES (pH = 7.5), 150 mM NaCl, 10 mM BME, and 5% glycerol). Gel filtration fractions were pooled and concentrated to 10 mg/mL before being flash-frozen in liquid nitrogen and stored at -80 °C until use [25].

2.2.2.2. In vitro ELISA-based kinase assay

Recombinantly expressed GST MEK-His, diluted in TTBS buffer (20 mM Tris (pH = 7.5), 150 mM NaCl, and 0.05% Tween 20) to 50 μg/mL in a volume of 100 μL, was bound to the wells of a 96-well glutathione-coated plate (Pierce Biotechnology). One microliter of compound (as racemic mixtures) with 2 serial dilutions in a 100% DMSO stock solution was added to a mixture of 50 μL of a buffer containing 50 mM HEPES (pH = 7.0) with 0.7 pmol of [V600E]BRAF kinase. This mixture was incubated at room temperature for 1 h before it was added to the GST-MEK-His-bound wells of the 96-well plate. An additional 50 μL of phosphorylation buffer (50 mM HEPES (pH = 7.0), 200 mM NaCl, 10 mM MgCl$_2$, and 200 μM ATP) was added to the well mixture to start the kinase reaction at 37 °C for 30 min. with intermittent shaking. The kinase reaction was stopped by extensive washing with TTBS buffer, and a 1:5000 dilution of anti-phospho-MEK1 (Ser218/222)/MEK2 (Ser222/226) monoclonal antibody (Millipore) in TTBS buffer was subsequently added to the wells and incubated for 1 h with shaking. Goat anti-rabbit IgG (H+L)-HRP conjugate (Bio-Rad Laboratories) in a 1:5000 dilution was added to the wells for incubation at room temperature with shaking. Finally, the Super Signal ELISA Pico chemiluminescent substrate (Pierce Biotechnology) was added to the wells. The luminescence signal was recorded with a luminescence filter using a Wallac 1420 luminometer (PerkinElmer) [25].

High throughput inhibitor screening was performed. Assays were conducted in glutathione coated 384-well plates and followed the procedures essentially as described above but using a 50 μL reaction volume instead of a 100 μL reaction volume to fit 384-well plate format. Specifically, GST-MEK protein diluted in TTBS to 50 μg/mL was dispensed into the wells of the glutathione coated 384-well plate to a final volume of 50 μL/well using a Matrix Wellmate Dispanser with a microplate stacker (Thermo Scientific). Each plate was agitated using an orbital shaker at 2500 rpm for 1 min. and incubated at room temperature for 1 h. Plates were aspirated and washed once using a wash program with vigorous agitation using an automated microplate washer (Biotek). 3.5

pico moles of [V600E]BRAF kinase domain diluted in 25 μL of 50 mM HEPES (4-(2-hydroxyethyl)-1-piperazineethanesulfonic acid)) pH = 7.5 buffer was added into each well of the plate using the Matrix Wellmate Dispanser, and 25 nl of individual compound (10 mM in 100% DMSO) was transferred into the solution using a Cybi-Well pin-transfer station (Cybio). Plates were agitated using an orbital shaker for 1 min and incubated at room temperature for 1 h. 25 μL of phosphorylation buffer was then added into the wells to start the kinase reaction (controls were tested to ensure the precise timing for the start of the kinase reaction). Kinase reactions were conducted at room temperature for 30 min and stopped by washing using the microplate washer. A 1:5000 dilution of Anti-phospho-MEK1 (Ser218/222)/MEK2 (Ser222/226) monoclonal antibody (Millipore) in TTBS buffer was subsequently dispensed into the wells to a final volume of 50 μl and incubated for 1 h with shaking. Goat anti-rabbit IgG (H+L)-HRP conjugate (BioRad Laboratories) in a 1:5000 dilution was then dispensed into the wells to a final volume of 50 μL to incubate at room temperature with agitation. Finally, 50 μL of the Super Signal ELISA Pico chemiluminescent substrate (Pierce Biotechnology) was dispensed into the wells to generate the chemiluminescence signal, which was detected using a 700 nm luminescence filter by an Envision chemiluminescence detector (PerkinElmer). A total of 31976 compounds were screened in duplicate including libraries of a diversity oriented synthesis (DOS), commercially available drug-like compounds, bioactive compounds, natural products, compounds collected from academic organic synthesis laboratories and a ChemBridge Kinase inhibitor biased library. Compounds were ranked based on a composite Z-score of both duplicates and the top 100 compounds were cherry-picked from the compound plates at the Broad Institute and they were re-analyzed by the same assay to confirm their inhibitory activities. According to the results, the top 23 compounds that were deemed to have drug-like properties were confirmed by reordering the compounds from their source vendors and confirming their inhibitor activities [25].

2.2.2.3. IC$_{50}$ value determination

For IC$_{50}$ calculations of the related quinolol and naphthol inhibitors, the same assay described above was used at different inhibitor concentrations to generate a sigmoidal dose response curve using [V600E]BRAF or [WT]BRAF protein. All dose response measurements were carried out in duplicate or triplicate and IC$_{50}$ values were derived from fitting the data to a sigmoidal dose response curve with a four-parameter logistic model using Graph Pad Prism [26].

IC$_{50}$ values were calculated using GraphPad Prism software (GraphPad Software, La Jolla, CA, USA). Data are reported as means±SEM and significance was calculated by Student's t-test using SPSS software (SPSS Inc., Paris, France). The concentrations range used were 0.01, 0.05, 0.1, 0.5 1, 5 and 10 μM.

2.3. Molecular docking

2.3.1. Docking procedure

Docking studies of all the synthesized compounds were performed by Molecular Operating Environment (MOE) [27]. The program operated under "Window 7" operating system installed on an Dell Pentium IV PC with a 2.8 MHz processor and 512 RAM. All minimizations were performed with MOE until a RMSD gradient of 0.05 Kcal/mol.Å with MMFF94 force field and the partial charges were automatically calculated. The score function, dock function (S, Kcal/mol) developed by MOE program was used for the evaluation of the binding affinity of the ligand.

2.3.2. Preparation of the target V600E BRAF kinase protein

The X-ray crystal structure of the enzyme with PLX3203, *N*-{2,4-difluoro-3-[(5-pyridin-3-yl-1*H*-pyrrolo[2,3-b]pyridin-3-yl)carbonyl]phenyl}ethanesulfonamide (PDB code: 4FK3) [28] was obtained from the protein data bank (www.rcsb.org) in PDB format. The enzyme was prepared for docking studies. (i) 3D protonation for the amino acid side chain and ligand. (ii) Deleting all water of crystallization away from the active site. (iii) Isolation of the active site, fixation to be dealt with as rigid structure and recognition of the amino acids. (iv) Creation of dummies around the active site. (v) Studying the interactions of the ligand with the amino acids of the active site.

2.3.3. Preparation of compounds for docking

The 3D structures of the synthesized compounds in addition to sorafenib (standard used for enzyme inhibition assay) were built using MOE and subjected to the following procedure: (i) 3D protonation of the structures. (ii) Running conformational analysis using systemic search. (iii) Selecting the least energetic conformer. (iv) Applying the same docking protocol used with ligand

2.3.4. Docking running

Prior to the docking of the pyridopyrazinone derivatives, redocking of the PLX3203 bound in the V600E BRAF active site was performed to validate the docking protocol. The generated most stable conformer of each compound was virtually docked into the predefined active site of V600E BRAF. The developed docked models were energetically minimized and then used to predict the interaction of the ligand with the amino acids in the active site of the enzyme.

3. Results and discussion

3.1. Chemistry

The target compounds **1**, **2**, **3a-j**, **4**, **5a-e**, **6a-d**, and **7a-c** were synthesized as depicted in Scheme 1. Condensation of 2,3-diaminopyridine with ethyl pyruvate in ethanol provided methylpyridopyrazinone, **1**. IR spectrum showed a band at 3186 cm^{-1} assigned to NH group and a band at 1685 cm^{-1} attributed to C=O group. ^{1}H NMR showed a singlet peak at δ 2.41 ppm assigned to CH$_3$ protons in addition to doublet, triplet and doublet at δ7.48, 7.67, 8.11 ppm, respectively, corresponding to pyridine protons. Bromomethyl compound **2** was achieved *via* bromination of compound **1** with bromine. Use of bromine in presence of sodium acetate in glacial acetic acid gave higher yield than bromination with *N*-bromo-succinamide [29]. ^{1}H NMR spectrum revealed disappearance of methyl protons singlet peak at δ 2.41 ppm and appearance of singlet peak at δ 3.10 ppm assigned to CH$_2$ protons. Mass spectrum showed both M$^+$ and M$^+$+2 at 240 and 242 *m/z*, respectively.

Refluxing bromomethyl compound **2** with different primary or secondary amines in ethanol afforded compounds **3a-j**. Catalytic amount of sodium iodide was used to accelerate the reaction [30]. IR spectra showed a band at 3421-3350 cm^{-1} corresponding to additional NH group for compounds **3d-i**. In addition, ^{1}H NMR spectra showed added aliphatic protons at δ 1.41-3.30 ppm for compounds **3a-c** or additional aromatic protons at δ 6.12-7.20 ppm for compounds **3d-j** and additional singlet peak at δ 10.09-11.61 ppm exchanged with D$_2$O corresponding to NH proton for compounds **3d-i**.

Refluxing bromomethyl compound **2** with hydrazine hydrate in ethanol afforded compound **4**. ^{1}H NMR spectrum showed additional two singlet peaks at δ 10.72 and 11.22 ppm exchanged with D$_2$O corresponding to added NH and NH$_2$ protons, respectively. Compounds **5a-e** were prepared *via*

reaction of hydrazino compound **4** with different appropriate aldehyde or ketone in glacial acetic acid. ^{1}H NMR spectra showed additional aromatic protons at δ 6.76-8.10 ppm in addition to signal at δ 8.10-8.19 ppm corresponding to benzylidene proton for compounds **5a-d**. Adopting cyclization with the aid of bromine and sodium acetate in glacial acetic acid at room temperature [31,32] for compounds **5a-d** afforded compounds **6a-d**. ^{1}H NMR spectra showed additional singlet signal at δ 5.82-6.21 ppm corresponding triazine proton.

Refluxing compound **4** with different cyclic acid anhydrides in glacial acetic acid provided compounds **7a-c**. ^{1}H NMR spectra showed additional triplet signal at δ 3.11 ppm assigned to CH$_2$-CH$_2$ protons for compound **7a** or a doublet signal at δ 5.11 ppm corresponding to CH=CH protons for compound **7b** or additional multiplet signal at δ 7.66-8.11 ppm attributed to added aromatic protons for compound **7c**.

3.2. Biological activity

3.2.1. Antitumor screening

Cell lines were provided by American Type Culture Collection (Rockville, MD). These cells were grown in RPMI-1640; all supplemented with 10% heat inactivated fetal bovine serum (FBS), 2 mM L-glutamine, and 1% penicillin-streptomycin. DMEM was also supplemented with 0.01 mg/mL insulin and 1 mM sodium pyruvate. Cells were incubated in a 5% CO$_2$ humidified incubator at 37 °C and passaged bi-weekly.

All the synthesized compounds were subjected to *in vitro* tumor growth inhibitory activity against eight different cell lines of human cancer cells. The cytotoxicity of the newly synthesized compounds against cancer cell lines *in vitro* was performed with the MTT assay according to the Mosmann's method [23]. The MTT assay is based on the reduction of the soluble 3-(4,5-methyl-2-thiazolyl)-2,5-diphenyl-2*H*-tetrazolium bromide (MTT) into a blue-purple formazan product, mainly by mitochondrial reductase activity inside living cells. Results were expressed in term of IC$_{50}$ [µM] (Table 1).

All newly synthesized compounds showed various activity against different cell lines compared with sorafenib. Compound **7c** showed good activity among the tested compounds against melanoma (LOXIMVI) cell line (IC$_{50}$ = 0.0045 µM) compared to sorafenib (IC$_{50}$ = 0.0034 µM). However, compounds **3c, d, j** were more active than sorafenib against ovarian cell line (OVCAR3) as they exhibited lower IC$_{50}$ (0.00456-0.043 µM) than that of sorafenib (0.12 µM). On the other hand, compounds **3b-f**, **5a**, **6b-d** and **7a-c** exhibited higher activity than sorafenib (IC$_{50}$ 0.17 µM) against thyroid cell line (CAL62) as they showed lower IC$_{50}$ (0.003-0.094 µM) while compounds **1** and **3j** showed comparable activity with sorafenib (IC$_{50}$ = 0.12 and 0.15 µM, respectively). Compounds **3g, j** and **5a** showed higher activity than sorafenib (IC$_{50}$ 0.006 µM) against thyroid cell line (FTC133) as they exhibited lower IC$_{50}$ (0.0032-0.0043 µM) while compound **3h** showed comparable activity with sorafenib at this cell line (0.0056 µM). In addition, compounds **3f** and **7b** were more active than sorafenib against thyroid cell line (BCPAP) as they exhibited lower IC$_{50}$ (0.08054 and 0.064 µM, respectively) compared to IC$_{50}$ of sorafenib (0.087 µM) while compounds **3d, e, 6d** and **7c** showed comparable activity with sorafenib against this cell line as they exhibited IC$_{50}$ (0.085-0.09 µM). Moreover, compounds **1**, **2**, **3a-d**, **4**, **5a,b**, **6b** and **7b,c** were more active than sorafenib against thyroid cell line (ML1) as revealed from lower IC$_{50}$ (0.10-0.58 µM) compared to IC$_{50}$ of sorafenib (0.61 µM) while compounds **3e,j** showed comparable activity with sorafenib against this cell line as they exhibited IC$_{50}$ (0.60 and 0.64 µM, respectively). On the other hand, compounds **3d-i** exhibited promising activity against colon cell lines HT29 and HCT116 than sorafenib as they exhibited much lower IC$_{50}$ (0.00032-0.00078 µM) compared to IC$_{50}$ of sorafenib (0.73 and 0.18 µM, respectively).

Table 1. *In vitro* growth inhibitory activity (IC$_{50}$, µM) against melanoma, thyroid, and ovarian cell lines.

Compound	Melanoma	Ovarian	Thyroid				Colon	
	LOXIMVI	OVCAR3	CAL62	FTC133	BCPAP	ML1	HT29	HCT116
1	1.45	1.34	0.12	0.21	0.13	0.17	1.23	*
2	2.67	2.35	0.32	0.26	0.24	0.26	5.43	7.66
3a	4.54	8.76	0.45	0.53	0.54	0.35	*	*
3b	6.34	3.56	0.09	0.68	0.67	0.28	8.78	4.56
3c	5.40	0.00456	0.0065	0.98	0.89	0.39	0.98	5.44
3d	0.023	0.043	0.0095	0.09	0.09	0.40	0.00034	0.00032
3e	6.43	9.39	0.075	0.09	0.09	0.60	0.00056	0.00056
3f	12.45	12.56	0.087	0.0098	0.08054	0.79	0.00032	0.00078
3g	34.43	34.56	0.43	0.0043	0.56	0.88	0.00035	0.00065
3h	0.13	23.56	0.57	0.0056	0.45	0.95	0.00043	0.00047
3i	0.43	5.67	0.63	0.0075	0.11	0.74	0.00047	0.00065
3j	0.35	0.034	0.15	0.0032	0.24	0.64	*	*
4	0.45	0.30	0.34	0.08	0.32	0.55	*	*
5a	0.45	0.234	0.003	0.0043	0.57	0.46	*	7.50
5b	0.45	0.45	0.436	0.034	0.68	0.57	0.098	7.60
5c	2.45	0.45	0.576	0.053	0.65	0.68	*	55.70
5d	5.78	5.49	0.605	0.072	0.34	0.70	*	32.60
5e	9.28	10.21	0.905	0.098	0.24	0.80	0.433	12.70
6a	3.29	10.11	0.874	0.0086	0.56	0.90	23.56	*
6b	5.69	23.56	0.094	0.99	0.78	0.10	3.67	*
6c	4.89	3.45	0.063	0.54	0.75	0.94	*	7.80
6d	9.08	6.034	0.033	0.37	0.086	0.75	*	23.60
7a	8.18	5.88	0.082	0.65	0.096	0.76	*	14.37
7b	0.065	2.12	0.082	0.47	0.064	0.58	*	16.54
7c	0.0045	7.13	0.011	0.38	0.085	0.57	*	17.67
Sorafenib	0.0034	0.12	0.17	0.006	0.087	0.61	0.73	0.18

* Inactive.

Table 2. IC$_{50}$ (95% confidence interval [nM]) of tested compounds for both ^{WT}BRAF and ^{V600E}BRAF.

Compound	IC$_{50}$ (95% Confidence Interval)^{WT}BRAF(nM)	IC$_{50}$ (95% Confidence Interval)^{V600E}BRAF (nM)
1	15.5	0.23
2	24.4	1.23
3a	36.5	0.45
3b	47.6	0.45
3c	58.5	1.45
3d	84.6	0.44
3e	73.5	0.47
3f	67.6	3.45
3g	58.7	3.45
3h	69.9	0.54
3i	78.8	0.65
3j	78.0	6.78
4	67.0	5.45
5a	46.6	0.56
5b	55.7	7.45
5c	44.5	0.34
5d	55.4	0.56
5e	66.5	0.34
6a	77.6	0.31
6b	88.7	0.28
6c	67.5	3.45
6d	56.6	7.65
7a	45.4	3.27
7b	56.5	4.30
7c	45.5	4.00
Sorafenib	37.8	0.48

Furthermore, compounds **5b,e** showed good activity (IC$_{50}$ = 0.098 and 0.433 µM, respectively) against colon cell lines HT29 (sorafenib IC$_{50}$ 0.73 µM). All tested compounds exhibited high activity against thyroid (CAL62, FTC133, BCPAP and ML1) cell lines. Compound **3d** exhibited potential activity against all tested cell lines.

3.2.2. *In vitro* kinase assay

The in vitro kinase assay of the synthesized compounds was investigated against both ^{WT}BRAF (BRAF kinase wild type) and ^{V600E}BRAF (mutant BRAF kinase) (Table 2). All compounds were highly active inhibitors for ^{V600E}BRAF (0.23-7.65 nM) compared with moderate activity against ^{WT}BRAF (15.5-88.7 nM).

Compounds **1**, **3a,b,d**, **5c,e**, and **6a,b** were more active than sorafenib as they exhibited lower IC$_{50}$ (0.23-0.45 nM) than that of sorafenib (0.48 nM). Compounds **3e,h,i**, and **5a,d** had comparable activity with sorafenib (0.47-0.65 nM). On the

other hand, compounds **2**, **3c,f,g,j**, **4**, **5b**, **6c,d** and **7a-c** were less active than sorafenib (1.23-7.65 nM).

3.3. Molecular docking

BRAF is isoform of RAF protein kinase (Rapidly Accelerated Fibrosarcoma), that was known at 1988. BRAF proteins are encoded by RAF oncogenes which are located in chromosome 7q32. BRAF is a serine/threonine specific protein kinase that has long been viewed as key players in the MAPK pathway. Under normal circumstances, BRAF is activated in a RAS small G-protein dependent manner. It then phosphorylates and activates the protein kinase MEK and ERK orderly, regulating gene expression and controlling how cells respond to extracellular signals.

BRAF kinase domain consists of two lobes, small N-terminal lobe and large C-terminal lobe. The small N-terminal lobe has antiparallel β-sheet structure which anchors and orients ATP molecule. The large C-terminal lobe is mainly α-helical which binds to MEK as a protein substrate.

Moreover, it contains a P-loop (glycine-rich ATP-phosphate-binding loop). The catalytic site is located between these two lobes that were occupied by most BRAF kinase inhibitors [33].

In each lobe (N and C-terminal lobes), a polypeptide segment is located which has both active and inactive conformations. In the small N-terminal lobe, a segment designated as αC-helix rotates and makes part of the active ATP- binding site. On the other hand, this activation segment in the large C-terminal lobe begins with a DFG (Asp/Phe/Gly) amino acid sequences and adjusted to make part of the ATP-binding site. In the inactive conformation of this segment in the large lobe, the phenylalanine side chain exposed away from the active site (DFG Asp-out conformation), while in the active conformation, the phenylalanine side chain rotates out and the aspartate side chains exposed into the binding sit [33].

Most BRAF kinase mutations occur in the activation segment (P-loop). These mutations keep the P-loop in the active state rather than the inactive state. The Val600Glu mutation (val 600 is replaced by glu in the P-loop) accounts for approximately 90% of known BRAF mutations which known as [V600E]BRAF kinase [33].

The X-ray crystal structure of BRAF with its PLX3203 (native ligand), *N*-{2,4-difluoro-3-[(5-pyridin-3-yl-1*H*-pyrrolo [2,3-b]pyridin-3-yl)carbonyl]phenyl}ethanesulfonamide(PDB code: 4FK3) [28] shows that it exists mainly in dimer form with binding to the DFG-out allosteric pocket of [V600E]BRAF kinase. The allosteric binding site is made accessible by a rearrangement of the activation loop and subsequent movement of a phenylalanine side chain out of a large hydrophobic pocket and into the ATP binding site. This movement results in a conformation that is mutually exclusive to ATP binding and also creates a large hydrophobic pocket to which the allosteric kinase inhibitors bind. In addition, H-bonding interactions with Cys532 in the ATP binding pocket which is necessary for tight binding of the inhibitor in the ATP-binding site and is present in most BRAF inhibitors [34].

The binding affinity of the ligand was evaluated with energy score (S, Kcal/mol) (Table 3). Low dock score energy indicates good affinity. Hydrogen bond, arene arene and arene cation interaction were also used to assess the binding models. The results of docking study; dock score, involved [V600E]BRAF kinase protein active site amino acid interacting ligand moieties and hydrogen bond length for each active compound and PLX3203 (Figure 2).
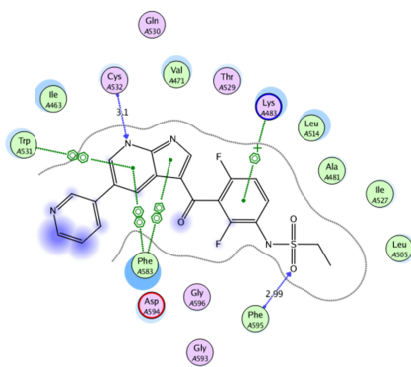

Figure 2. 2D interaction of PLX3203with [V600E]BRAF.

Analysis of the docking results revealed that:

(i) The PLX3203-([V600E]BRAF) complex was precisely reproduced by the docking procedure as demonstrated by low root mean square deviation, RMSD (1.2173) and dock score (-19.2870 kcal/mol, Table 3), achieved that the docking protocol was valid. PLX3203 nearly fits in the active site forming two hydrogen bonding interactions with Cys 532 and

Phe 595, three arene arene interactions with Phe 583 and Trp 531 and one arene cation interaction with Lys 483 (Figure 2).

(ii) The docking score for sorafenib (standard used for enzyme inhibition assay) was -23.4155 Kcal/mol. Sorafenib fits in the active site forming one hydrogen bond with Asp 594 and one arene arene interaction with Phe 583 (Figure 3).
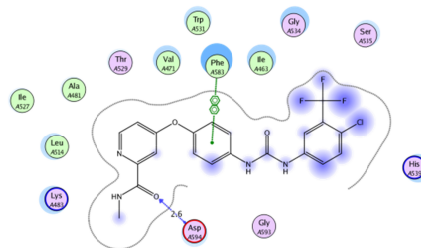

Figure 3. 2D interaction of sorafenib with [V600E]BRAF.

(iii) The docking score of tested compounds were all in the range -10.6210 to -21.0419 Kcal/mol. All compounds showed one or two hydrogen bonds and/ or arene arene or arene cation interactions with the enzyme active site residues. Only compounds **3j** and **7a** showed no binding interaction with active site although binding scores were -15.8120 and -14.6555 respectively. Lys 483, Trp 531, Cys 532, Gly 534, Phe 583, Asp 594 and Phe 595 are the amino acids residue involved in these interactions.

(iv) The docking scores of compounds **3a-j** (-10.6210 to -19.0422 Kcal/mol) with IC_{50} (0.44-6.78 nM). In addition, compounds **5a-e** showed docking scores in the range -13.3412 to -21.0419 Kcal/mol while their IC_{50} were 0.34-7.45 nM. Moreover, the docking scores of compounds **6a-d** (-14.6422 to -17.4771 Kcal/mol), with IC_{50} (0.28 to 7.65 nM). Furthermore, compounds **7a-c** showed docking scores -14.6555 to -18.1910 Kcal/mol and IC_{50} 3.27-4.30 nM.

(v) Compound **5d**gave best docking score (-21.0419 Kcal/mol) and binds with 2 hydrogen bonds (3.12 and 3.37 Å) with Asp 594 and Lys 483 respectively, one arene arene interaction with Trp 531 and one arene cation interaction with Lys 483 (Figure 4).
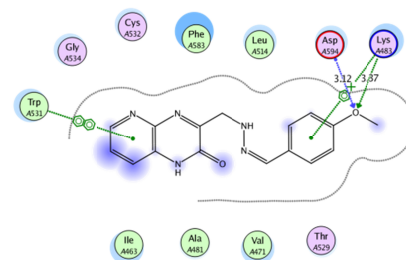

Figure 4. 2D interaction of compound **5d** with [V600E]BRAF.

Compound **1**, most active compound gave best IC_{50} (0.23 nM) while gave a docking score of -11.3281 Kcal/mol and bind with the active site with one hydrogen bond with Cys 532 and one arene arene interaction with Phe 583. Compound **6b**, second most active compound exhibited good IC_{50} (0.28 nM) and showed a docking score of -16.0553 Kcal/mol which bind to active site with one arene atene interaction with Lys 483 and one arene cation interaction with Phe 583.

4. Conclusion

A number of new pyridopyrazinone derivatives were synthesized. Most of these compounds have a significant activity towards thyroid cell lines rather than rest of other cell lines. Compound **3d** was the most active one.

Table 3. Docking results.

Compound	Energy score S (Kcal/mol)	Amino acids interaction	Interacting groups	Hydrogen bond length (Å)
PLX3203	-19.2870	Lys 483 (arene cation)	Phenyl ring	
		Trp 531 (arene arene)	N Pyridine	
		Cys 532	N Pyridine	3.1
		Phe 583 (arene arene)	N Pyridine	
		Phe 583 (arene arene)	N Pyrrole	
		Phe 595	SO$_2$	2.99
Sorafenib	-23.4155	Phe 583 (arene arene)	Phenyl ring	
		Asp 594	C=O	2.6
1	-11.3281	Cys 532	N Pyridine	3.02
		Phe 583 (arene arene)	Pyridine ring	
2	-13.0101	Cys 532	N Pyridine	3.05
		Phe 583 (arene arene)	Pyridine ring	
3a	-13.2439	Cys 532	C=O	2.69
		Phe 583 (arene arene)	Pyridine ring	
3b	-10.6210	Lys 483 (arene cation)	Pyridine ring	
		Phe 583 (arene cation)	Piperidine ring	
		Asp 594	N Pyridine	2.98
3c	-11.6002	Cys 532	C=O	3.13
		Phe 583 (arene arene)	Pyridine ring	
3d	-17.5978	Cys 532	NH Piperazine	2.27
		Cys 532	C=O	2.69
3e	-17.7071	Lys 483 (arene cation)	Phenyl ring	
3f	-16.0602	Cys 532	NH Piperazine	1.83
		Cys 532	C=O	3.22
3g	-18.4843	Cys 532	NH Piperazine	2.2
		Cys 532	C=O	2.61
3h	-18.2255	Cys 532	NH Piperazine	2.26
		Cys 532	C=O	2.56
3i	-19.0422	Cys 532	NH Piperazine	2.24
		Cys 532	C=O	2.58
3j	-15.8120	-	-	-
4	-12.0174	Cys 532	C=O	2.57
		Gly 534	NH$_2$	1.94
		Phe 583 (arene arene)	Pyridine ring	
5a	-16.5954	Lys 483 (arene cation)	Phenyl ring	
		Cys 532	NH Piperazine	1.83
		Cys 532	C=O	2.52
5b	-16.7560	Lys 483 (arene cation)	Pyridine ring	
		Asp 594	N Pyridine	2.63
5c	-13.3412	Cys 532	NH Piperazine	1.86
		Cys 532	C=O	2.57
5d	-21.0419	Lys 483 (arene cation)	Phenyl ring	
		Lys 483	OCH$_3$	3.37
		Trp 531 (arene arene)	Pyridine ring	
		Asp 594	OCH$_3$	3.12
5e	-18.4503	Lys 483 (arene cation)	Pyridine ring	
		Asp 594	N Pyridine	2.64
6a	-14.6422	Cys 532	C=O	2.53
		Phe 583 (arene arene)	Pyridine ring	
6b	-16.0553	Lys 483 (arene cation)	Phenyl ring	
		Phe 583 (arene arene)	Pyridine ring	
6c	-15.7831	Cys 532	NH Piperazine	1.58
6d	-17.4771	Lys 483	OCH$_3$	2.99
7a	-14.6555	-	-	-
7b	-17.4101	Lys 483 (arene cation)	Pyridine ring	
		Asp 594	N Pyridine	2.65
7c	- 18.1910	Lys 483 (arene cation)	Pyridine	
		Asp 594	N Pyridine	2.66

It exhibited promising activity against all tested cell lines. In addition, the *in vitro* kinase assay revealed that the tested compounds were more active towards [V600E]BRAF rather than [WT]BRAF enzyme. The docking study revealed binding of most compounds with Cys 532 at the active site. Finally, based on both *in vitro* and docking studies, introduction of unsubstituted, *o*-CH$_3$, *p*-Cl, *p*-Br phenyl amino group increased activity of [V600E]BRAF inhibitors (compounds **3d,e,h,i**). Also Shiff's compounds with unsubstituted benzylidine increased activity, while *p*-substituted benzylidine ring with electron withdrawing group decreased activity of these inhibitors (compounds **5d**,**e**). In case of tricyclic derivatives; substitution with Cl at position 4 increased activity (compound **6b**). Although the docking study showed non-significant correlation with results of enzyme inhibition assay, most of docked compounds shared some of binding interactions with [V600E]BRAF active sites similar to those of native ligand

(PLX3203). This suggests that these compounds might possibly act as [V600E]BRAF inhibitors.

References

[1].   Gupta, S. *Chem. Rev.* **1994**, *94 (6)*, 1507-1551.
[2].   Sparano, J. A. , In Molecular Targeting in Oncology, Springer: 2008, pp 55-73.
[3].   Sebolt-Leopold, J. S.; Herrera, R. *Nat. Rev. Cancer* **2004**, *4(12)*, 937-947.
[4].   Zebisch, A.; Troppmair, J. *Cell. Mol. Life Sci. CMLS* **2006**, *63(11)*, 1314-1330.
[5].   Wan, P. T.; Garnett, M. J.; Roe, S. M.; Lee, S.; Niculescu-Duvaz, D.; Good, V. M.; Project, C. G.; Jones, C. M.; Marshall, C. J.; Springer, C. J. *Cell* **2004**, *116(6)*, 855-867.
[6].   Davies, H.; Bignell, G. R.; Cox, C.; Stephens, P.; Edkins, S.; Clegg, S.; Teague, J.; Woffendin, H.; Garnett, M. J.; Bottomley, W. *Nature* **2002**, *417(6892)*, 949-954.
[7].   Garnett, M. J.; Marais, R. *Cancer cell* **2004**, *6(4)*, 313-319.

[8]. Dibb, N. J.; Dilworth, S. M.; Mol, C. D. *Nat. Rev. Cancer* **2004**, *4(9)*, 718-727.
[9]. Cohen, Y.; Xing, M.; Mambo, E.; Guo, Z.; Wu, G.; Trink, B.; Beller, U.; Westra, W. H.; Ladenson, P. W.; Sidransky, D. J. *Cancer Inst. Natl.* **2003**, *95(8)*, 625-627.
[10]. Xu, X.; Quiros, R. M.; Gattuso, P.; Ain, K. B.; Prinz, R. A. *Cancer Res.* **2003**, *63(15)*, 4561-4567.
[11]. Lee, J. H.; Lee, E. S.; Kim, Y. S. *Cancer* **2007**, *110(1)*, 38-46.
[12]. Hong, D. S.; Vence, L.; Falchook, G.; Radvanyi, L. G.; Liu, C.; Goodman, V.; Legos, J. J.; Blackman, S.; Scarmadio, A.; Kurzrock, R. *Clin. Cancer Res.* **2012**, *18(8)*, 2326-2335.
[13]. Gray-Schopfer, V.; Wellbrock, C.; Marais, R. *Nature* **2007**, *445(7130)*, 851-857.
[14]. Whittaker, S.; Menard, D.; Kirk, R.; Ogilvie, L.; Hedley, D.; Zambon, A.; Lopes, F.; Preece, N.; Manne, H.; Rana, S. *Cancer Res.* **2010**, *70(20)*, 8036-8044.
[15]. Hoeflich, K. P.; Gray, D. C.; Eby, M. T.; Tien, J. Y.; Wong, L.; Bower, J.; Gogineni, A.; Zha, J.; Cole, M. J.; Stern, H. M. *Cancer Res.* **2006**, *66(2)*, 999-1006.
[16]. Karasarides, M.; Chiloeches, A.; Hayward, R.; Niculescu-Duvaz, D.; Scanlon, I.; Friedlos, F.; Ogilvie, L.; Hedley, D.; Martin, J.; Marshall, C. J. *Oncogene* **2004**, *23(37)*, 6292-6298.
[17]. Eisen, T.; Ahmad, T.; Flaherty, K.; Gore, M.; Kaye, S.; Marais, R.; Gibbens, I.; Hackett, S.; James, M.; Schuchter, L. *Br. J. Cancer* **2006**, *95(5)*, 581-586.
[18]. Wilhelm, S. M.; Carter, C.; Tang, L.; Wilkie, D.; McNabola, A.; Rong, H.; Chen, C.; Zhang, X.; Vincent, P.; McHugh, M. *Cancer Res.* **2004**, *64(19)*, 7099-7109.
[19]. Ratain, M. J.; Eisen, T.; Stadler, W. M.; Flaherty, K. T.; Kaye, S. B.; Rosner, G. L.; Gore, M.; Desai, A. A.; Patnaik, A.; Xiong, H. Q. *J. Clin. Oncol.* **2006**, *24(16)*, 2505-2512.
[20]. King, A. J.; Patrick, D. R.; Batorsky, R. S.; Ho, M. L.; Do, H. T.; Zhang, S. Y.; Kumar, R.; Rusnak, D. W.; Takle, A. K.; Wilson, D. M. *Cancer Res.* **2006**, *66(23)*, 11100-11105.
[21]. El-Nassan, H. B. *Eur. J. Med. Chem.* **2014**, *72*, 170-205.
[22]. Liao, J. J. L. *J. Med. Chem.* **2007**, *50 (3)*, 409-424.
[23]. Mosmann, T. *J. Immunol. Methods* **1983**, *65(1)*, 55-63.
[24]. Hansen, M. B.; Nielsen, S. E.; Berg, K. *J. Immunol. Methods* **1989**, *119(2)*, 203-210.
[25]. Qin, J.; Xie, P.; Ventocilla, C.; Zhou, G.; Vultur, A.; Chen, Q.; Liu, Q.; Herlyn, M.; Winkler, J.; Marmorstein, R. *J. Med. Chem.* **2012**, *55(11)*, 5220-5230.
[26]. Kim, J. E.; Leung, E.; Baguley, B. C.; Finlay, G. J. *Front. Genet.* **2013**, *4(97)*, 1-8.
[27]. Molecular Operating Environment (MOE), Chemical Computing Group, Canada, https://www.chemcomp.com/MOE-Molecular_Operating_Environment.htm.
[28]. Tsai, J.; Lee, J. T.; Wang, W.; Zhang, J.; Cho, H.; Mamo, S.; Bremer, R.; Gillette, S.; Kong, J.; Haass, N. K. *Proc. Natl. Acad. Sci.* **2008**, *105(8)*, 3041-3046.
[29]. Leese, C.; Rydon, H. *J. Chem. Soc.* **1955**, 303-309.
[30]. Bahadur, S.; Pandey, K. *Indian Chem. Soc.* **1980**, *57(4)*, 447-448.
[31]. Westphal, G.; Wasicki, H.; Zielinski, U.; Weber, F.; Tonew, M.; Tonew, E. *Pharmazie* **1977**, *32(10)*, 570.
[32]. Tarzia, G.; Occelli, E.; Toja, E.; Barone, D.; Corsico, N.; Gallico, L.; Luzzani, F. *J. Med. Chem.* **1988**, *31(6)*, 1115-1123.
[33]. Roskoski, R. *Biochem. Biophys. Res. Commun.* **2010**, *399(3)*, 313-317.
[34]. Wang, X.; Kim, J. *J. Med. Chem.* **2012**, *55(17)*, 7332-7341.